

## RESEARCH ARTICLE

# Quantifying the acid–base status of dragonflies across their transition from breathing water to breathing air

Daniel J. Lee\* and Philip G. D. Matthews

## ABSTRACT

Amphibiotic dragonflies show a significant increase in hemolymph total CO<sub>2</sub> (TCO<sub>2</sub>) as they transition from breathing water to breathing air. This study examined the hemolymph acid–base status of dragonflies from two families (Aeshnidae and Libellulidae) as they transition from water to air. CO<sub>2</sub> solubility ( $\alpha_{\text{CO}_2}$ ) and the apparent carbonic acid dissociation constant ( $pK_{\text{app}}$ ) were determined *in vitro*, and pH/bicarbonate concentration ( $[\text{HCO}_3^-]$ ) plots were produced by equilibrating hemolymph samples with  $P_{\text{CO}_2}$  between 0.5 and 5 kPa in custom-built rotating microtonometers. Hemolymph  $\alpha_{\text{CO}_2}$  varied little between families and across development (mean  $0.355 \pm 0.005 \text{ mmol l}^{-1} \text{ kPa}^{-1}$ ) while  $pK_{\text{app}}$  was between 6.23 and 6.27, similar to values determined for grasshopper hemolymph. However, the non-HCO<sub>3</sub><sup>−</sup> buffer capacity for dragonfly hemolymph was uniformly low relative to that of other insects ( $3.6\text{--}5.4 \text{ mmol l}^{-1} \text{ pH}^{-1}$ ). While aeshnid dragonflies maintained this level as bimodally breathing late-final instars and air-breathing adults, the buffer capacity of bimodally breathing late-final instar *Libellula* nymphs increased substantially to  $9.9 \text{ mmol l}^{-1} \text{ pH}^{-1}$ . Using the  $\text{pH}/[\text{HCO}_3^-]$  plots and *in vivo* measurements of TCO<sub>2</sub> and  $P_{\text{CO}_2}$  from early-final instar nymphs, it was calculated that the *in vivo* hemolymph pH was 7.8 for an aeshnid nymph and 7.9 for a libellulid nymph. The  $\text{pH}/[\text{HCO}_3^-]$  plots show that the changes in acid–base status experienced by dragonflies across their development are more moderate than those seen in vertebrate amphibians. Whether these differences are due to dragonflies being secondarily aquatic, or arise from intrinsic differences between insect and vertebrate gas exchange and acid–base regulatory mechanisms, remains an open question.

**KEY WORDS:** Acid–base balance, Ontogeny, Odonata, Rectal gill, Respiratory acidosis, Evolution

## INTRODUCTION

The changes in blood acid–base balance that occur when an animal transitions from breathing water to breathing air were first established from studies on vertebrates – in particular, the amphibians and air-breathing fish that switch between these two respiratory media during their lifetime (e.g. Erasmus et al., 1970; Garey and Rahn, 1970; Just et al., 1973; Lenfant and Johansen, 1968). However, while numerous invertebrates also move routinely between water and air, the respiratory and acid–base consequences of this behavior have been well characterized only among the decapod crustaceans (e.g. Howell et al., 1973; Truchot, 1975). As


both vertebrates and crustaceans are ancestrally aquatic, their transition from water to air represents a shift from their ancestral state to a derived condition. In contrast, although insects are an ancestrally terrestrial group, members of at least 12 of the ~30 insect orders have independently evolved the ability to live and breathe underwater as juveniles (Balian et al., 2008; Wootton, 1988). Thus, these amphibiotic insects provide a valuable opportunity to learn how terrestrial animals have modified their respiratory systems and acid–base balance to function underwater over evolutionary time, and what physiological changes occur as they transition back to breathing air during their development. Lee et al. (2018) examined how hemolymph total carbon dioxide (TCO<sub>2</sub>) content changes during development in the amphibiotic dragonflies (Odonata, Anisoptera). The water-to-air respiratory transition of a dragonfly proceeds in stages. Nymphs begin their life as water breathers, using only their tidally ventilated rectal gill to exchange gases with the environment (Tillyard, 1915). However, immediately before metamorphosis, the late-final instar nymphs become bimodal breathers, developing functional mesothoracic spiracles to breathe air while continuing to breathe water using their rectal gill (Corbet, 1962; Gaino et al., 2007). Finally, the adult dragonflies emerge from their final-instar exuviae, shedding their rectal gill in the process, and begin breathing air exclusively through their spiracles (Tillyard, 1915). Studying the change in hemolymph TCO<sub>2</sub> content across these developmental stages revealed that the water-to-air respiratory transition of aeshnid and libellulid dragonflies is accompanied by a much smaller increase in hemolymph TCO<sub>2</sub> (45–48%) compared with the increase experienced by vertebrates (up to 445%) making the same respiratory transition (Lee et al., 2018). The finding that water-breathing dragonfly nymphs have an unusually high hemolymph TCO<sub>2</sub> was unexpected, and is possibly due to their secondarily derived water-breathing capabilities and, presumably, an unusually low water-convection requirement.

The observation that TCO<sub>2</sub> increases significantly as a dragonfly nymph approaches metamorphosis begs the question: what is happening to the acid–base status of the hemolymph? The hemolymph acid–base status describes the equilibrium between CO<sub>2</sub> partial pressure ( $P_{\text{CO}_2}$ ), bicarbonate concentration  $[\text{HCO}_3^-]$  and pH, and can reveal whether these parameters change passively or are defended by active pH regulatory mechanisms across the water-to-air transition. However, there is a paucity of information regarding the acid–base status of insect hemolymph generally, let alone for amphibiotic insects, and the few measurements available in the literature are restricted to a small number of species (Matthews, 2017). Therefore, studying the hemolymph acid–base status of dragonflies not only provides further insight into how amphibiotic insects transition between two respiratory media but also expands our knowledge of insect respiratory and acid–base physiology more generally.

To quantify the hemolymph acid–base status of dragonflies across development, the hemolymph CO<sub>2</sub> solubility and apparent

Department of Zoology, University of British Columbia, Vancouver, BC, Canada V6T 1Z4.

\*Author for correspondence (danlee@zoology.ubc.ca)

 D.J.L., 0000-0002-6287-8172; P.G.D.M., 0000-0003-0682-8522

Received 10 July 2019; Accepted 23 October 2019

dissociation constant of carbonic acid ( $pK_{app}$ ) were measured in aeshnid and libellulid dragonflies at multiple developmental stages, from pre-final instar nymphs to adults. Hemolymph samples were extracted and equilibrated with various levels of  $P_{CO_2}$  using a custom-built microtonometer setup before pH and  $[HCO_3^-]$  were measured. From this information, non- $HCO_3^-$  blood buffer lines and  $P_{CO_2}$  isopleths were calculated to describe and compare the acid–base status of dragonfly hemolymph as they develop from water-breathing nymphs to air-breathing adults.

## MATERIALS AND METHODS

### Animals

Aeshnid and libellulid dragonflies and nymphs were captured in and around ponds at the University of British Columbia, Point Grey campus. They were housed and identified as described previously (Lee et al., 2018). The adult aeshnid dragonflies were identified as *Anax junius* (Drury 1773) and *Aeshna multicolor* Hagen 1861. Pre-, early- and late-final instar nymphs of *A. junius* were also collected and identified. However, only a very few *A. multicolor* nymphs were collected and, thus, they could not be used for analysis. Libellulid dragonflies were classified as early- and late-final *Libellula quadrimaculata* Linnaeus 1758 and *Libellula forensis* Hagen 1861. However, these nymphs could only be identified to species level after hemolymph collection. As the small volumes of hemolymph collected from these nymphs necessitated combining them for analysis, this resulted in some pooled samples being a mix of the two species. Therefore, it was decided to analyze *L. quadrimaculata* and *L. forensis* together as early- and late-final *Libellula*. Unfortunately, adult *L. quadrimaculata* and *L. forensis* could not be included in this study because of difficulties in obtaining sufficient hemolymph for analysis.

### Preparation of hemolymph samples

#### Dragonfly nymphs

Hemolymph was obtained from dragonfly nymphs using the same protocol as described in Lee et al. (2018). However, for this study a 22s-gauge 25  $\mu$ l Hamilton syringe with its needle lumen primed with distilled water was used to extract the hemolymph. Priming the syringe added 1.13  $\mu$ l of distilled water to the hemolymph sample per extraction, resulting in the sample being diluted by 12%. However, this dilution was unavoidable as priming was necessary to remove the air from the needle lumen, as well as to prevent clogging of the syringe. Hemolymph was collected into an ice-cooled 1.5 ml Eppendorf tube to minimize clotting, and was centrifuged at 1520  $g$  for 10 min to separate any cellular and tissue debris from the supernatant.

#### Dragonfly adults

Dragonfly adults were restrained on an expanded polystyrene sheet as described previously (Lee et al., 2018), then the 8th abdominal tergite was removed using a razor blade and scissors to expose the underlying hemocoel (Heinrich and Casey, 1978). The gut and heart were pushed to the side using an insect pin, and the hemolymph from the wound was then slowly aspirated into a length of 30-gauge PTFE tubing connected to a 26s-gauge 10  $\mu$ l Hamilton syringe. The hemolymph was then collected into an Eppendorf tube and processed as described above. Subsequent handling of the hemolymph using a primed syringe resulted in the final analyzed sample being diluted by 7% with distilled water.

### Hemolymph $CO_2$ solubility

To calculate hemolymph  $CO_2$  solubility ( $\alpha_{CO_2}$ ), 30  $\mu$ l of hemolymph was collected from an individual insect. This was

then centrifuged as described above, then 20  $\mu$ l of the supernatant was removed and placed in a 6 mm $\times$ 50 mm test tube together with 20  $\mu$ l of 0.1 mol l<sup>-1</sup> HCl. The hemolymph–HCl solution always had a pH below 3, indicating that all  $HCO_3^-$  had been converted to  $CO_2$  (Harrison, 1988). A micro-combination pH electrode mounted in a 16 gauge hypodermic needle (MI-414B, Microelectrodes Inc., Bedford, NH, USA) was used for all pH measurements. It was connected to a pH amplifier (FE165, ADInstruments, Colorado Springs, CO, USA) and a PowerLab analog-to-digital converter (PL3504, ADInstruments). The pH electrode was calibrated using three pH standards (pH 4.00 $\pm$ 0.01, 7.00 $\pm$ 0.01, 10.00 $\pm$ 0.01), and pH measurements were recorded using Labchart (v.8.1.10400.0, ADInstruments).

A custom-made microtonometer, 3D printed from ABS plastic filament, was used to equilibrate the hemolymph–HCl sample with gas mixtures of known  $P_{CO_2}$  (Fig. 1). The microtonometer was capable of rotating two test tubes simultaneously, and consisted of a 1000:1 geared-down DC electric motor (Micrometal Gearmotor no. 1596, Pololu, Las Vegas, NV, USA) that turned a 24 mm diameter wheel with two grooves around its perimeter. An elastic band in each groove looped around the middle of a test tube, which was loosely clamped in a frame beneath the motor mount. The motor caused the test tube to rotate in place at 42 rpm, allowing the hemolymph–HCl mixture to smear across the inner wall. Mixing of the sample was further enhanced by the passive tumbling of a 7 $\times$ 2 mm PTFE-coated stir bar placed into each test tube. During equilibration, the microtonometer was held at an angle of  $\sim$ 20 deg from horizontal with the test tubes partly submerged in a water bath that was temperature controlled to 20°C (F33-ME, Julabo, Seelbach, Baden-Württemberg, Germany). Two 0–500 ml min<sup>-1</sup> mass flow controllers (MC500SCCM-D/5M, Alicat Scientific, Tucson, AZ, USA) were controlled by gas mixing software (Flow Vision v.1.3.13.0, Alicat Scientific) to combine 99.998%  $N_2$  and 100%  $CO_2$  compressed gases (Praxair, Mississauga, ON, Canada) into a 20 kPa  $P_{CO_2}$  gas mixture flowing at a combined total flow rate of 400 ml min<sup>-1</sup> STPD. Flow rates were verified using a Bios DryCal Definer 220-L primary flow meter that had been calibrated using NIST standards (Mesa Laboratories, Inc., Lakewood, CO, USA). The 20 kPa gas mixture was split into four streams using an air-line aquarium manifold (Accuair 4-way aquarium gang valve, J. W. Pet Company Inc., Arlington, TX, USA), and each stream was humidified by bubbling it through a 2 ml volume of 20°C water before being delivered to the surface of the hemolymph–HCl mixture by a length of 21 gauge Tygon tubing. The microtonometer motor was connected to a 6 V DC power supply, and the hemolymph–HCl mixture was equilibrated with the 20 kPa  $P_{CO_2}$  gas mixture for 30 min. The time required for a sample to fully equilibrate was determined empirically using hemolymph solutions. Initial tests recording the pH change of a 70  $\mu$ l sample of hemolymph showed that it was fully equilibrated with 0.5 kPa  $P_{CO_2}$  within 30 min. As 70  $\mu$ l was the largest volume and 0.5 kPa was the lowest  $P_{CO_2}$  used in this study, 30 min was deemed sufficient time for full equilibration of all samples. After equilibration, the test tube was removed from the microtonometer and slotted into a holding rack inside the 20°C water bath. The gas line was placed back into the tube to continue flushing the headspace with the same 20 kPa  $P_{CO_2}$  gas mixture, while the top of the tube was loosely plugged with a cotton ball to hold the tube in position and prevent outside air from reaching the hemolymph sample. A 5  $\mu$ l sample of the  $CO_2$ -equilibrated hemolymph–HCl mixture was extracted and analyzed for  $TCO_2$  using the protocol outlined in Lee et al. (2018). Briefly, compressed  $N_2$  from a gas

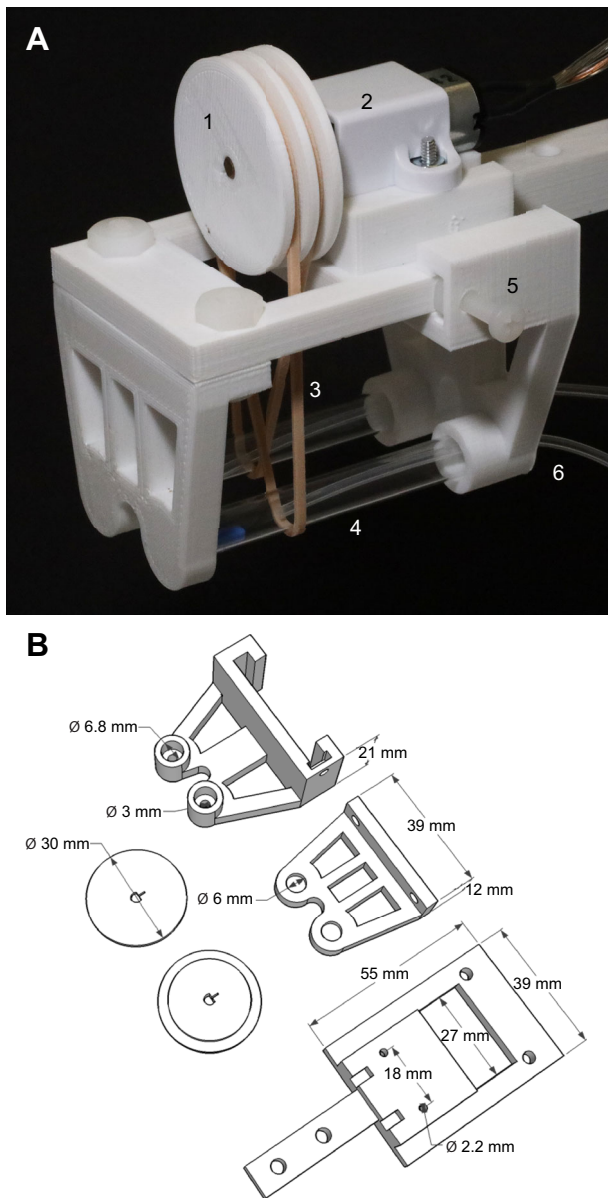


**Fig. 1. The 3D printed microtonometer.** (A) The assembled view shows the test tubes (4) used to equilibrate 40–70  $\mu\text{l}$  samples of hemolymph clamped beneath the motor (2) and motor mount. Elastic bands (3) couple the test tubes to the drive wheel (1), while tubing inserted through the top of the test tube clamp (6) allows the test tube to be continually purged with the desired gas mixture. A screw (5) holds the removable part of the test tube clamp in place during operation. (B) Schematic diagram showing the dimensions of the individual 3D printed components.  $\varnothing$ , diameter.

cylinder (99.998% pure, Praxair) was regulated at a flow rate of 20  $\text{ml min}^{-1}$  STPD through a 0–100  $\text{ml min}^{-1}$  mass flow controller (MC100SCCM-D/5M, Alicat Scientific). This  $\text{N}_2$  stream then passed through cell A of a two-channel LI-7000 infra-red  $\text{CO}_2$  gas analyzer (LI-COR, Lincoln, NE, USA) to provide a constant zero  $\text{CO}_2$  reference. It then flowed through a custom-made gas sparging column that consisted of a cylindrical glass chamber (4.7 ml internal volume), bubbling up through an acid solution [1 ml of 0.01  $\text{mol l}^{-1}$  HCl mixed with 1  $\mu\text{l}$  Antifoam 204 (Sigma-Aldrich, St Louis, MO, USA)] to prevent excessive frothing during sample injections. After passing through the acid solution, the  $\text{N}_2$  gas and any liberated

gaseous  $\text{CO}_2$  was passed through cell B of the infra-red  $\text{CO}_2$  gas analyzer for analysis. Injecting a 5  $\mu\text{l}$  hemolymph sample into the sparging column through the gas-tight injection port with a PTFE-lined septum resulted in a bolus of  $\text{CO}_2$  being liberated and flushed through the infra-red  $\text{CO}_2$  gas analyzer. The area-under-the-curve (AUC) function in the statistical software R v.3.5.0 (<http://www.R-project.org/>) was used to calculate the volume of liberated  $\text{CO}_2$  ( $\text{TCO}_2$ ). To ensure the accuracy of these measurements, a series of sodium bicarbonate standard solutions (10, 15, 20, 25 and 30  $\text{mmol l}^{-1}$ ) was prepared weekly and run before and after each measurement.

The measured  $\text{TCO}_2$  ( $\text{mmol l}^{-1}$ ) and known  $P_{\text{CO}_2}$  (kPa) were used to calculate  $\text{CO}_2$  solubility using Henry's law:

$$\alpha_{\text{mix}} = [\text{TCO}_2]/P_{\text{CO}_2}, \quad (1)$$

where  $\alpha_{\text{mix}}$  is the  $\text{CO}_2$  solubility of the hemolymph–HCl mixture.

The above process was repeated 3 times using 40  $\mu\text{l}$  samples of the 0.1  $\text{mol l}^{-1}$  HCl used to acidify the hemolymph samples, as both a technical replication and to calculate the  $\text{CO}_2$  solubility of this acid solution. Finally, the following equation was used to calculate the true hemolymph  $\text{CO}_2$  solubility:

$$\alpha_{\text{hemo}} = f_{\text{hemo}}^{-1}(\alpha_{\text{mix}} - f_{\text{HCl}}\alpha_{\text{HCl}}), \quad (2)$$

where  $f_{\text{hemo}}$  and  $f_{\text{HCl}}$  are the fractions of hemolymph and HCl in the mixture, respectively (Harrison, 1988). The same protocol was used for all dragonfly nymphs and adults; however, for *A. multicolor*, 30  $\mu\text{l}$  of hemolymph was pooled from two individuals as it was not possible to obtain the required volume from a single adult.

### **pK<sub>app</sub>**

#### **Dragonfly nymphs**

The protocol for calculating the  $\text{pK}_{\text{app}}$  of hemolymph was similar to that used to calculate hemolymph  $\alpha_{\text{CO}_2}$  (above), with the following differences. An 80  $\mu\text{l}$  sample of hemolymph was collected from an individual, and 68  $\mu\text{l}$  of the centrifuged supernatant was placed in a test tube. Then, 2  $\mu\text{l}$  of 0.7  $\text{mol l}^{-1}$  NaF was added to the hemolymph to inhibit any enzymes or reactions that could spontaneously alter pH (Harrison, 1988). The test tube was placed into the microtonometer setup. The two mass flow controllers were used to combine 99.998%  $\text{N}_2$  and 5%  $\text{CO}_2$  balance  $\text{N}_2$  compressed gases (Praxair) to create 0.5, 1, 2, 3, 4 and 5 kPa  $P_{\text{CO}_2}$  gas mixtures. The hemolymph sample was equilibrated to each  $P_{\text{CO}_2}$  for 30 min, and following the equilibration period at each  $P_{\text{CO}_2}$ , both pH and the  $\text{TCO}_2$  content were measured. The pH electrode described previously was inserted directly into the test tube to measure pH. Afterwards, the electrode was removed and 5  $\mu\text{l}$  of the hemolymph was analyzed for  $\text{TCO}_2$  as described previously (Lee et al., 2018). The pH,  $\text{TCO}_2$ ,  $\alpha_{\text{CO}_2}$  and  $P_{\text{CO}_2}$  were used to calculate  $\text{pK}_{\text{app}}$  using a rearrangement of the Henderson–Hasselbalch equation:

$$\text{pK}_{\text{app}} = \text{pH} - \log_{10} \frac{[\text{TCO}_2] - \alpha P_{\text{CO}_2}}{\alpha P_{\text{CO}_2}}. \quad (3)$$

The above protocol was used for all dragonfly nymphs. Hemolymph from pre-, early- and late-final *A. junius* was collected from single individuals. However, hemolymph from two individuals was pooled for the early- and late-final *Libellula* measurements because of their substantially smaller size.

#### **Dragonfly adults**

The same protocol as above was used for adult dragonflies; however, 60  $\mu\text{l}$  of hemolymph was pooled from two *A. junius*, while



60 µl was pooled from three *A. multicolor*, and 48.6 µl of the supernatant was mixed with 1.4 µl of 0.7 mol l<sup>-1</sup> NaF. Only 0.5, 1, 3 and 5 kPa  $P_{\text{CO}_2}$  was tested because of the limited volume of hemolymph available for analysis in these samples.

### Relationship between $pK_{\text{app}}$ and pH

It is generally accepted that blood  $pK_{\text{app}}$  is dependent on blood pH in vertebrates and crustaceans (Boutilier et al., 1984). As one of the objectives of this study was to quantify the  $pK_{\text{app}}$  of dragonfly hemolymph for comparison with vertebrate and crustacean values, it was necessary to assess whether such a relationship exists in dragonflies. In order to test for a significant effect of pH on  $pK_{\text{app}}$ ,  $pK_{\text{app}}$  was first calculated at each experimental  $P_{\text{CO}_2}$  for all measured hemolymph samples from a particular species and developmental stage. The calculated  $pK_{\text{app}}$  values for all samples were then plotted against their respective pH on a single graph, and a linear model was fitted to the data to test for a significant relationship between these two variables.

### pH/ $\text{HCO}_3^-$ diagram

#### Non- $\text{HCO}_3^-$ blood buffer line

To generate the non- $\text{HCO}_3^-$  blood buffer line, data collected from the  $pK_{\text{app}}$  experiment were used. For each dragonfly species and life stage, the  $\text{TCO}_2$  measured at each experimental  $P_{\text{CO}_2}$  was first converted to  $\text{HCO}_3^-$  using the following equation (Davenport, 1969):

$$[\text{HCO}_3^-] = [\text{TCO}_2] - \alpha P_{\text{CO}_2}. \quad (4)$$

Then, the calculated  $\text{HCO}_3^-$  and their corresponding pH values were averaged to find the mean  $\text{HCO}_3^-$  and pH for each experimental  $P_{\text{CO}_2}$ . Linear regressions were fitted to these data to produce the buffer lines, and the non- $\text{HCO}_3^-$  buffer capacity was taken to be the slope of this line.

#### $P_{\text{CO}_2}$ isopleth

$P_{\text{CO}_2}$  isopleths were also generated using data from the  $pK_{\text{app}}$  experiment, and the rearranged Henderson–Hasselbalch equation:

$$[\text{HCO}_3^-] = 10^{\text{pH} - pK_{\text{app}}} \times \alpha P_{\text{CO}_2}. \quad (5)$$

For each experimental  $P_{\text{CO}_2}$ ,  $\text{HCO}_3^-$  was calculated across a pH range of 7 to 8.3, and these sets of  $[\text{HCO}_3^-]$  against pH were plotted for each experimental  $P_{\text{CO}_2}$  to generate the isopleths.

### Statistical analyses

Data were analyzed in R v.3.5.0 (<http://www.R-project.org/>). A one-way ANOVA was performed to test for any statistical differences between the hemolymph  $\alpha_{\text{CO}_2}$  of dragonflies. Linear models were fitted to the  $pK_{\text{app}}$  versus pH data to test for any statistical relationships between these variables, and were also fitted to the  $\text{HCO}_3^-$  versus pH data to visualize the non- $\text{HCO}_3^-$  blood buffer lines and calculate the buffer capacities for the different dragonfly groups. Analysis of covariance (ANCOVA) was performed to test for any statistical differences between the slopes of the non- $\text{HCO}_3^-$  blood buffer lines of dragonflies. Data are shown as means  $\pm$  s.e.m. unless otherwise stated.

## RESULTS

### Hemolymph $\alpha_{\text{CO}_2}$

Hemolymph  $\alpha_{\text{CO}_2}$  was determined for samples of hemolymph from early- and late-final *A. junius* nymphs, *A. junius* and *A. multicolor* adults, early- and late-final *Libellula*, as well as for the solution of 0.1 mol l<sup>-1</sup> HCl (Table 1). The hemolymph  $\alpha_{\text{CO}_2}$  of pre-final *A. junius* nymphs could not be measured because of a lack of animals; however, statistical analysis showed that there were no significant differences between the hemolymph  $\alpha_{\text{CO}_2}$  of any of the dragonflies, nymph or adult, aeshnid or libellulid (one-way ANOVA,  $F=1.397$ , d.f.=5,  $P=0.3$ ). Therefore, the mean of all dragonfly hemolymph  $\alpha_{\text{CO}_2}$  was calculated as  $0.355 \pm 0.005$  mmol l<sup>-1</sup> kPa<sup>-1</sup>, and this value was used as the hemolymph  $\alpha_{\text{CO}_2}$  of pre-final *A. junius*.

### $pK_{\text{app}}$

Measurements of  $pK_{\text{app}}$  were made on pre-, early- and late-final *A. junius* nymphs, *A. junius* and *A. multicolor* adults, and early- and late-final *Libellula*. Pre-final *A. junius* nymphs, *A. multicolor* adults, and early- and late-final *Libellula* nymphs showed a significant relationship between pH and  $pK_{\text{app}}$ . Therefore, the equation of the line was calculated for the above four groups, while mean  $pK_{\text{app}}$  values were calculated for early- and late-final *A. junius* nymphs and adults (Table 1).

### Acid–base status

Comparison of the non- $\text{HCO}_3^-$  buffer capacities of *A. junius* (Fig. 2), *A. multicolor* (Fig. 3) and *Libellula* spp. (Fig. 4) showed that pre-final

**Table 1. Mean hemolymph  $\alpha_{\text{CO}_2}$  and  $pK_{\text{app}}$  across development for the studied dragonflies**

Species and developmental stage	$\alpha_{\text{CO}_2}$ (mmol l <sup>-1</sup> kPa <sup>-1</sup> ) (n)	$pK_{\text{app}}$ (n)
<i>Anax junius</i> pre-final nymph	NA*	$=0.11 \times \text{pH} + 5.40$ (6)
<i>Anax junius</i> early-final nymph	$0.363 \pm 0.004$ (4)	$6.24 \pm 0.02$ (6)
<i>Anax junius</i> late-final nymph	$0.358 \pm 0.007$ (5)	$6.27 \pm 0.02$ (6)
<i>Anax junius</i> adult	$0.373 \pm 0.005$ (3)	$6.23 \pm 0.02$ (4)
<i>Aeshna multicolor</i> adult	$0.321 \pm 0.035$ (3)	$=0.07 \times \text{pH} + 5.48$ (3)
<i>Libellula</i> early-final nymph	$0.351 \pm 0.013$ (5)	$= -0.06 \times \text{pH} + 6.74$ (6)
<i>Libellula</i> late-final nymph	$0.361 \pm 0.008$ (6)	$=0.14 \times \text{pH} + 5.20$ (6)
Mean	$0.355 \pm 0.005$ (26)**	NA*
0.1 mol l <sup>-1</sup> HCl	$0.390 \pm 0.003$ (3)	NA*
<i>Melanoplus bivittatus</i> <sup>a</sup>	0.34	6.24
<i>Gastrophilus intestinalis</i> <sup>b</sup>	NA*	$6.08$ (38°C), $6.19$ (16°C)

$\alpha_{\text{CO}_2}$ ,  $\text{CO}_2$  solubility;  $pK_{\text{app}}$ , apparent carbonic acid dissociation constant. The mean is given for all species and developmental stages. Data for 0.1 mol l<sup>-1</sup> HCl and for two other insect species are shown for comparison. Values are shown either as means  $\pm$  s.e.m. or as linear regressions where applicable. All values were obtained at 20°C, unless otherwise stated.

\*Values were not measured, not applicable or not provided. \*\*There were no significant differences between any of the hemolymph  $\alpha_{\text{CO}_2}$  values (one-way ANOVA,  $F=1.397$ , d.f.=5,  $P=0.3$ ).

<sup>a</sup>*Melanoplus bivittatus* data from Harrison (1988). <sup>b</sup>*Gastrophilus intestinalis* data from Levenbook (1950a).

*A. junius* nymphs had a value of  $5.4 \text{ mmol l}^{-1} \text{ pH}^{-1}$ , which was not significantly different from the buffer capacities of both early- and late-final *A. junius* nymphs ( $3.6$  and  $5.8 \text{ mmol l}^{-1} \text{ pH}^{-1}$ , respectively) (Fig. 5). *Anax junius* and *A. multicolor* adults had a buffer capacity of  $4.8$  and  $5.8 \text{ mmol l}^{-1} \text{ pH}^{-1}$ , respectively, neither of which was significantly different from that of any of the *A. junius* nymphs. Early-final *Libellula* nymphs had a buffer capacity that was not significantly different from that of all Aeshnidae ( $5.3 \text{ mmol l}^{-1} \text{ pH}^{-1}$ ) but this was significantly lower than the value for late-final *Libellula* ( $9.9 \text{ mmol l}^{-1} \text{ pH}^{-1}$ ) (Fig. 6), which had the highest buffer capacity of all comparison groups (ANCOVA,  $F=13.767$ , d.f.=6,  $P<0.001$ ).

### Verification of experimental protocol

As a custom-built microtonometer system was used in this study, it was necessary to ensure that our apparatus and  $\text{CO}_2$ -measurement technique produced accurate values that were comparable to those found by others. The solubility of  $\text{CO}_2$  in a  $0.1 \text{ mol l}^{-1} \text{ HCl}$  solution measured here ( $0.390 \pm 0.003 \text{ mmol l}^{-1} \text{ kPa}^{-1}$ ; Table 1) is in excellent agreement with values previously reported for other HCl solutions at  $20^\circ\text{C}$ :  $0.39 \text{ mmol l}^{-1} \text{ kPa}^{-1}$  in  $1.0 \text{ mol l}^{-1} \text{ HCl}$  (Bridges and Scheid, 1982) and  $0.38 \text{ mmol l}^{-1} \text{ kPa}^{-1}$  in  $0.001 \text{ mol l}^{-1} \text{ HCl}$  (Harrison, 1988).

### DISCUSSION

#### Hemolymph acid-base status

Findings from the aeshnid dragonflies (Figs 2, 3 and 5) show that at any given  $P_{\text{CO}_2}$ , the hemolymph  $[\text{HCO}_3^-]$  of late-final *A. junius* nymphs is always higher than that of the pre- and early-final *A. junius* nymphs, and is instead very similar to that of the air-breathing adults. This is in good agreement with previous measurements of hemolymph  $\text{TCO}_2$  in these species, which showed that the  $\text{TCO}_2$  of late-final *A. junius* nymphs was not significantly different from that of the air-breathing adults (Lee et al., 2018), indicating that the hemolymph acid-base status of late-final nymphs is more like that of an air breather rather than that of a water breather. This can be explained by the observation that late-final instar nymphs of both aeshnid and libellulid dragonflies are not exclusively water breathers, but develop the ability to breathe air even while continuing to use their rectal gills (Corbet, 1962; Gaino et al., 2007; de Pennart and Matthews, 2019). The data also show that the hemolymph pH of late-final nymphs is more alkaline at any given  $P_{\text{CO}_2}$  compared with that of early-final nymphs (Fig. 5). A higher hemolymph  $[\text{HCO}_3^-]$  and pH at a given  $P_{\text{CO}_2}$  may indicate a metabolic compensation in response to a respiratory acidosis (Truchot, 1975); however, without knowing the *in vivo* hemolymph  $P_{\text{CO}_2}$  and pH from late-final nymph and adult dragonflies, it is difficult to assess whether the air-breathing life stages maintain a constant pH or allow it to change during the respiratory transition. Future studies will aim to obtain *in vivo* measurements of  $P_{\text{CO}_2}$  and pH across dragonfly development in order to determine whether air-breathing dragonfly late-final nymphs and adults exist in a fully or partially compensated state of respiratory acidosis, relative to early-final nymphs.

Despite the increase in hemolymph  $[\text{HCO}_3^-]$  during the respiratory transition of dragonflies, the non- $\text{HCO}_3^-$  blood buffer capacity of *A. junius* did not show any statistical differences between developmental stages (Fig. 5). This indicates that the hemolymph of water-breathing pre- and early-final nymphs, the bimodally breathing late-final nymphs, and air-breathing adults is equally resistant to changes in respiratory  $\text{CO}_2$ . However, this is not the case for the *Libellula* nymphs (Figs 4 and 6), which show a significant

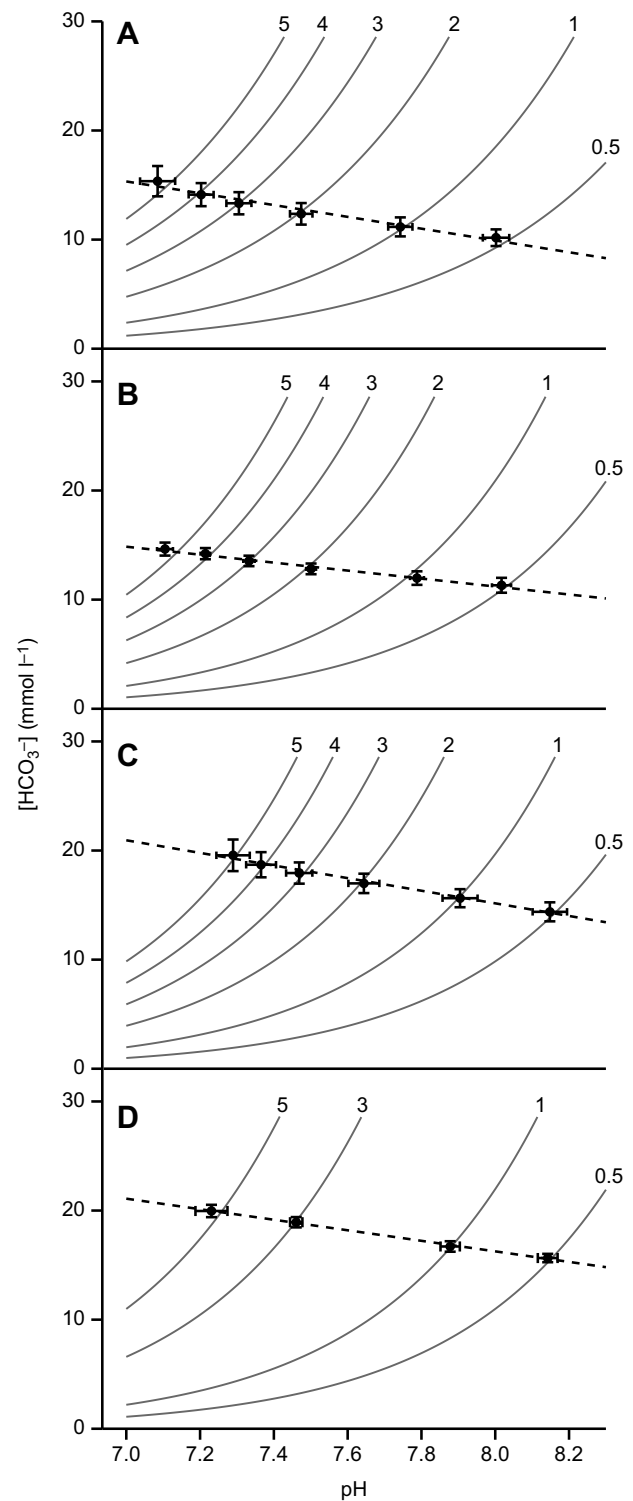


**Fig. 2. *Anax junius* hemolymph bicarbonate concentration as a function of pH.** Hemolymph samples collected from pre-final (A;  $n=6$ ), early-final (B;  $n=6$ ) and late-final (C;  $n=6$ ) nymphs and adult (D;  $n=4$ ) dragonflies. Filled circles represent the mean *in vitro* pH and bicarbonate concentration ( $[\text{HCO}_3^-]$ ) values at a given  $P_{\text{CO}_2}$ , while the dashed linear regressions represent the corresponding non- $\text{HCO}_3^-$  blood buffer lines. The buffer lines were calculated and positioned based on the series of *in vitro* pH and  $[\text{HCO}_3^-]$  measurements for each dragonfly comparison group. Gray curved lines are  $P_{\text{CO}_2}$  isopleths (kPa) calculated using the Henderson–Hasselbalch equation and experimentally determined apparent carbonic acid dissociation constant ( $pK_{\text{app}}$ ). Vertical and horizontal error bars represent s.e.m. for  $[\text{HCO}_3^-]$  and pH, respectively.

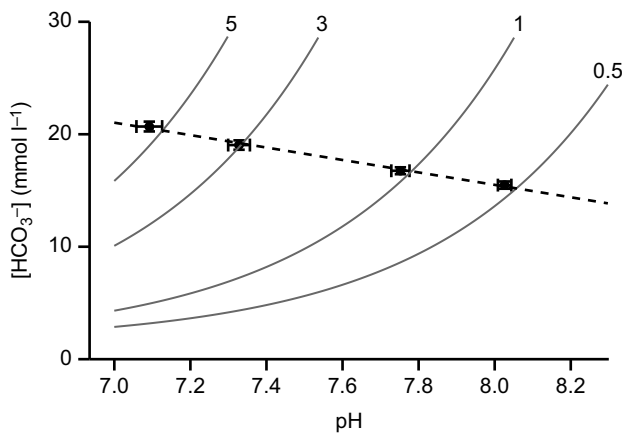


**Fig. 3.** Adult *Aeshna multicolor* hemolymph  $[\text{HCO}_3^-]$  as a function of pH ( $n=3$ ). Filled circles represent the mean *in vitro* pH and  $[\text{HCO}_3^-]$  values at a given  $P_{\text{CO}_2}$ , while the dashed linear regression represents the corresponding non- $\text{HCO}_3^-$  blood buffer line. Gray curved lines are  $P_{\text{CO}_2}$  isopleths (kPa) calculated using the Henderson–Hasselbalch equation and experimentally determined  $pK_{\text{app}}$ . Vertical and horizontal error bars represent s.e.m. for  $[\text{HCO}_3^-]$  and pH, respectively.

increase in buffer capacity as the nymphs transition from water-breathing early-final nymphs to bimodally breathing late-final nymphs. This indicates that the hemolymph of late-final *Libellula* is

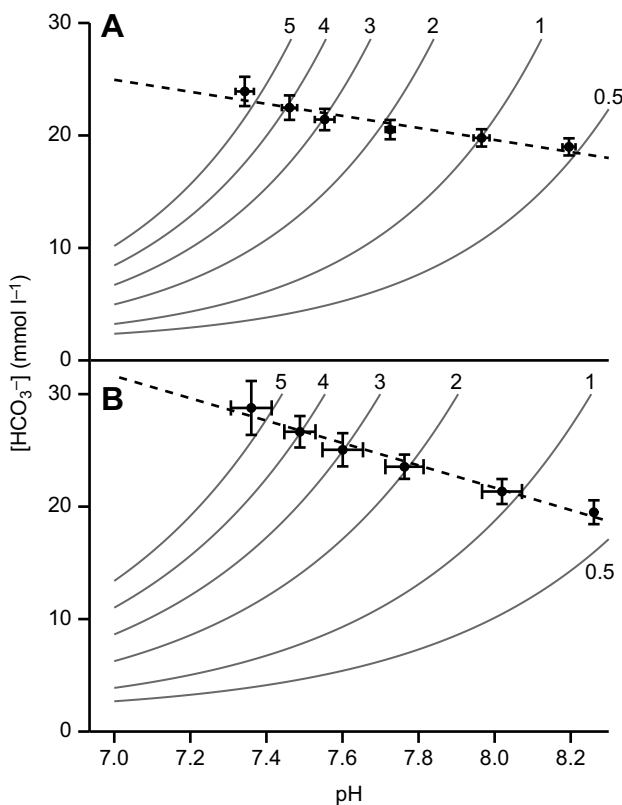


**Fig. 4.** Libellulid hemolymph  $[\text{HCO}_3^-]$  as a function of pH. Hemolymph samples collected from early-final (A;  $n=6$ ) and late-final (B;  $n=6$ ) nymphs. Filled circles represent the mean *in vitro* pH and  $[\text{HCO}_3^-]$  values at a given  $P_{\text{CO}_2}$ , while dashed linear regressions represent the corresponding non- $\text{HCO}_3^-$  blood buffer lines. Gray curved lines are  $P_{\text{CO}_2}$  isopleths (kPa) calculated using the Henderson–Hasselbalch equation and experimentally determined  $pK_{\text{app}}$ . Vertical and horizontal error bars represent s.e.m. for  $[\text{HCO}_3^-]$  and pH, respectively.

more resistant to respiratory acidosis than that of early-final nymphs. The non- $\text{HCO}_3^-$  buffer capacity is typically attributed to the presence of proteins and organic acids (Harrison, 2001; Levenbook, 1950b), but without measuring how the composition and concentration of various proteins and other organic molecules change during development in dragonflies, the basis for the difference in non- $\text{HCO}_3^-$  buffer capacity of *Libellula* nymphs remains unknown. That libellulid dragonfly nymphs change their hemolymph chemistry differently to the aeshnid dragonflies is in agreement with the large differences in  $\text{TCO}_2$  recorded between these families at all developmental stages: adult *L. quadrimaculata* and *L. forensis* dragonflies possess a hemolymph  $\text{TCO}_2$  that is significantly higher than that of all aeshnid life stages, both nymph and adult (Lee et al., 2018).

### Dragonflies compared with other animals

Perhaps the most striking finding of the current study is that the hemolymph acid–base status of dragonfly hemolymph across their water-to-air transition lies midway between the blood bicarbonate values that occur across the lifecycle of a vertebrate amphibian: water-breathing dragonfly nymphs have much higher hemolymph  $[\text{HCO}_3^-]$  than water-breathing tadpoles, but the terrestrial adult dragonflies have a  $[\text{HCO}_3^-]$  that is far lower than that of air-breathing frogs (Figs 5 and 6). Despite these differences in  $[\text{HCO}_3^-]$ , it can be shown using the *in vivo*  $P_{\text{CO}_2}$  value of 0.9 kPa measured from early-final aeshnid nymphs that the pH of this nymph's hemolymph must be  $\sim 7.8$ , essentially indistinguishable from the blood pH of a water-breathing tadpole (Erasmus et al., 1970) or crab (Truchot, 1975). Thus, aeshnid dragonfly nymphs appear to be maintaining a hemolymph pH which is not dissimilar from that of other aquatic animals, but are maintaining a higher internal  $[\text{HCO}_3^-]$  and  $P_{\text{CO}_2}$ . Unfortunately, the *in vivo* pH or  $P_{\text{CO}_2}$  measurements necessary to calculate libellulid *in vivo* pH are currently lacking. However, hemolymph  $\text{TCO}_2$  has been measured in early-final *L. quadrimaculata* nymphs, and this is a reasonable proxy for  $[\text{HCO}_3^-]$ , given that even at a  $P_{\text{CO}_2}$  of 5 kPa, the current data indicate that 93% of the  $\text{TCO}_2$  exists as  $\text{HCO}_3^-$ . Using this  $19.6 \pm 1.0 \text{ mmol l}^{-1}$  value (Lee et al., 2018), the *in vivo* pH of the early-final *Libellula* nymphs in this study would be  $\sim 7.9$ , only slightly more alkaline than estimated for *A. junius*. However, this is substantially higher than the mean hemolymph pH of  $7.58 \pm 0.074$  measured from 'final' instar *Libellula julia* nymphs (Rockwood and Coler, 1991), which could set the lower bound for a reasonable *in vivo* hemolymph pH for a libellulid nymph.

Calculating the non- $\text{HCO}_3^-$  buffer capacities from amphibians and crustaceans shows that these values change very little between the water-breathing and air-breathing life stages in both lineages. In *Rana catesbeiana*, the blood buffer capacity for both tadpoles and frogs is  $\sim 9.5 \text{ mmol l}^{-1} \text{ pH}^{-1}$  (Erasmus et al., 1970), while for *Carcinus maenas* crabs moving between water and air, the buffer capacity is also similar ( $\sim 13$  to  $13.3 \text{ mmol l}^{-1} \text{ pH}^{-1}$ ; Truchot, 1975). The stability of these buffer values indicates that the compensation of a respiratory acidosis during the transition from water breathing to air breathing is mainly achieved by increasing  $\text{HCO}_3^-$  in the blood (Truchot, 1975), rather than by changing the non- $\text{HCO}_3^-$  buffer system. *Anax junius* and adult *A. multicolor* show the same trend, indicating that these dragonflies also mainly rely on metabolic compensation during their water-to-air transition. *Libellula* nymphs, however, appear to use both the  $\text{HCO}_3^-$  and the non- $\text{HCO}_3^-$  buffer systems to defend hemolymph pH in the face of elevated hemolymph  $P_{\text{CO}_2}$ , which is unlike what has been observed in vertebrates and crustaceans.

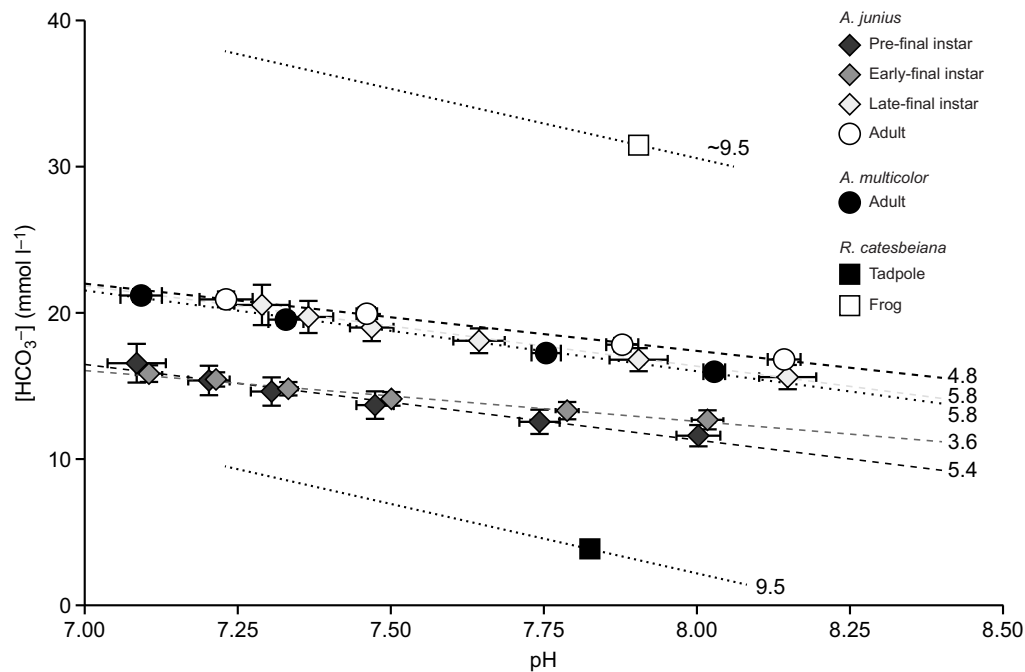


**Fig. 5. Changes in Aeshnidae hemolymph  $[\text{HCO}_3^-]$  as a function of pH across development from a water-breathing nymph to an air-breathing adult.** Diamonds and circles represent the mean *in vitro* pH and  $[\text{HCO}_3^-]$  values at a given  $P_{\text{CO}_2}$  (0.5, 1, 2, 3, 4, 5 kPa, right to left), while dashed lines and adjacent numbers indicate non- $\text{HCO}_3^-$  buffer capacity ( $\text{mmol l}^{-1} \text{pH}^{-1}$ ). For comparison, non- $\text{HCO}_3^-$  buffer lines for a water-breathing tadpole and air-breathing bullfrog (*Rana catesbeiana*) are shown; squares indicate *in vivo* blood pH (data from Erasmus et al., 1970). Vertical and horizontal error bars represent s.e.m. for  $[\text{HCO}_3^-]$  and pH, respectively.

Comparison of the non- $\text{HCO}_3^-$  buffer capacities of dragonflies with those measured from other insects shows that they are noticeably lower. The highest buffer capacity of late-final *Libellula* is only two-thirds of the average value found in grasshoppers, locusts, moth pupae and fly larvae (Harrison, 2001). It may be that these other flying species lack the impressive autoventilation ability of dragonflies (Weis-Fogh, 1967), resulting in larger changes in internal  $P_{\text{CO}_2}$  between rest and activity. In addition, many of these species also display discontinuous gas exchange patterns (Buck and Friedman, 1958; Harrison et al., 1995) or live in hypercapnic environments (Levenbook, 1950a), both of which are expected to elevate their hemolymph  $P_{\text{CO}_2}$  intermittently. Under such circumstances, the hemolymph would require higher buffer

capacity to prevent changes in pH due to the respiratory  $\text{CO}_2$ , and this may explain the comparatively high non-bicarbonate buffer values in these species.

#### Hemolymph $\alpha_{\text{CO}_2}$ and $\text{pK}_{\text{app}}$

Studies on the acid–base physiology in insects often make the assumption that the  $\text{CO}_2$  solubility and dissociation constants measured from the hemolymph of one species are sufficiently similar to be substituted for those of another (e.g. Gulinson and Harrison, 1996; Harrison, 1989). However, in the absence of additional data, this assumption had not been well tested. This study is the first to provide these constants for an amphibiotic insect lineage, in an attempt to fully describe the hemolymph acid–base

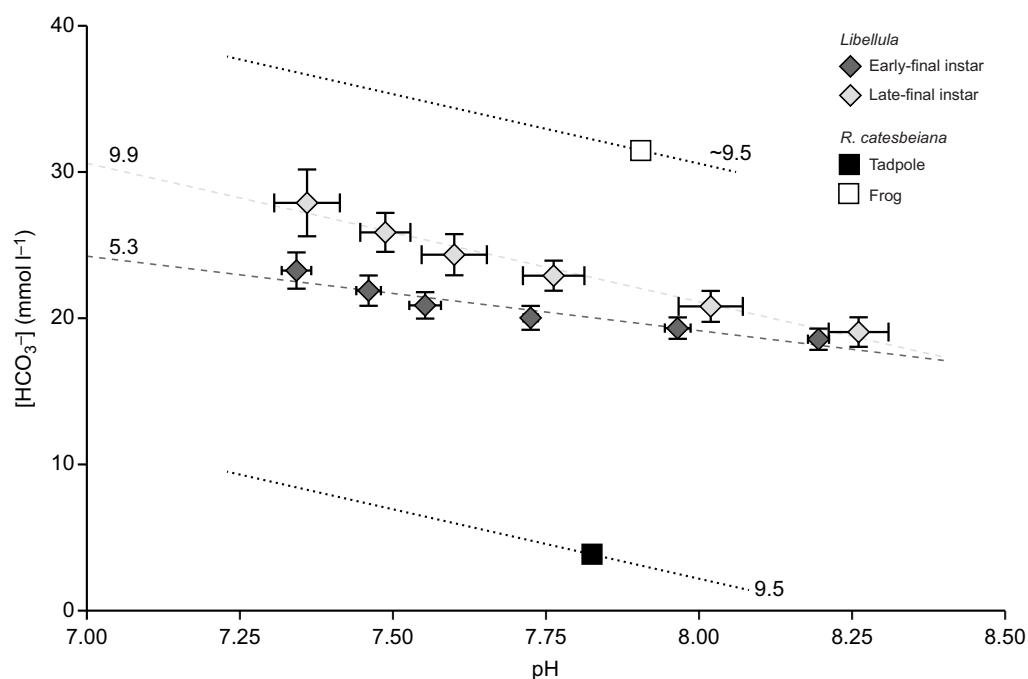


**Fig. 6. Changes in hemolymph  $[\text{HCO}_3^-]$  as a function of pH across development to bimodal gas exchange as late-final instars in libellulid dragonfly nymphs.** Dashed lines and adjacent numbers indicate non- $\text{HCO}_3^-$  buffer capacity ( $\text{mmol l}^{-1} \text{pH}^{-1}$ ). For comparison, non- $\text{HCO}_3^-$  buffer lines for a water-breathing tadpole and air-breathing bullfrog (*Rana catesbeiana*) are shown; squares indicate *in vivo* blood pH (data from Erasmus et al., 1970). Vertical and horizontal error bars represent s.e.m. for  $[\text{HCO}_3^-]$  and pH, respectively.



status of dragonflies without relying on constants derived from distantly related species. The data presented here indicate that hemolymph  $\alpha_{\text{CO}_2}$  does not change appreciably during a dragonfly's water-to-air transition. As hemolymph temperature was held constant during these measurements, it follows that the only other parameter that could influence  $\text{CO}_2$  solubility, hemolymph ionic strength or composition (Boutilier et al., 1984), did not change sufficiently between the aquatic and terrestrial life stages to alter solubility. Measurement of the composition of *L. quadrimaculata* hemolymph shows that its salt concentration (expressed as an equivalent NaCl solution) increases from 170 mmol l<sup>-1</sup> in the final-instar nymph to 247 mmol l<sup>-1</sup> in the mature adult (Nicholls, 1983), which would cause  $\text{CO}_2$  solubility to decrease by a trivial 0.007 mmol l<sup>-1</sup> kPa<sup>-1</sup> (Heisler, 1986). Comparison of  $\alpha_{\text{CO}_2}$  values calculated from these two previous hemolymph salt concentrations using the equations given by Heisler (1986) and more recently Stabenau and Heming (1993), with the mean  $\alpha_{\text{CO}_2}$  values for early- and late-final *Libellula* nymphs, shows very good agreement: the calculated value for unspecified 'final' instar nymphs is 5.2% higher than the measured value for early-final nymphs, but the calculated value for the adult dragonfly is within 0.5% of the measured late-final nymph's value. A hemolymph molarity of 206 mmol l<sup>-1</sup> measured from *Aeshna grandis* and 195 mmol l<sup>-1</sup> from *Aeshna cyanea* nymphs, some of which were 'final instar' (Sutcliffe, 1962), give  $\alpha_{\text{CO}_2}$  values that are only 0.8% and 1% higher, respectively, than that reported here for early final *A. junius* nymphs. The measured  $\alpha_{\text{CO}_2}$  values in the hemolymph of dragonfly nymphs and adults are also in good agreement with values determined for grasshoppers and locusts, with *Melanoplus bivittatus* having a hemolymph  $\alpha_{\text{CO}_2}$  of 0.34 mmol l<sup>-1</sup> kPa<sup>-1</sup> at 20°C (see Table 1), which is similar to values determined for vertebrate plasma (Harrison, 1988). Thus, the current data support the general trend that plasma/hemolymph  $\alpha_{\text{CO}_2}$  is similar across a wide variety of animal lineages for a given temperature and ionic strength.

The  $\text{pK}_{\text{app}}$  of carbonic acid calculated from early-, late-final and adult *A. junius* in this study (6.23–6.27) brackets that obtained from *M. bivittatus* (6.24 at 20°C; Harrison, 1988), and the range of  $\text{pK}_{\text{app}}$  calculated from pre-final *A. junius*, and early- and late-final *Libellula* also overlaps with these values. These results show that the  $\text{pK}_{\text{app}}$  of dragonfly hemolymph is similar across water- and air-breathing life stages, as well as between families. However, it is surprising that pH does not appear to have a consistent effect on  $\text{pK}_{\text{app}}$  in the above dragonfly groups, as data from vertebrates indicate either a non-linear (Boutilier et al., 1984) or a negative linear relationship (Iversen et al., 2012) between pH and  $\text{pK}_{\text{app}}$ . Three of the *A. junius* groups do not show pH dependence of  $\text{pK}_{\text{app}}$ , and while pre-final *A. junius*, adult *A. multicolor*, and early- and late-final *Libellula* show a statistically significant effect of pH on  $\text{pK}_{\text{app}}$ , only early-final *Libellula* shows the same negative trend as described previously (Boutilier et al., 1984; Iversen et al., 2012). These results are in contrast to those reported previously from vertebrates, as well as with the observation that pH does not affect  $\text{pK}_{\text{app}}$  in grasshoppers and locusts (Harrison, 1988). However, while the relationship between  $\text{pK}_{\text{app}}$  and pH may be statistically significant for the data presented here, it remains to be seen whether it is biologically relevant.

## Conclusions

The number of insects that have adapted to living and breathing underwater is vast, yet we are only just beginning to understand the respiratory and acid–base physiology of these animals. The aquatic nymphs of both dragonfly families studied here show very similar

non- $\text{HCO}_3^-$  buffer capacities, although  $[\text{HCO}_3^-]$  is higher in the libellulid nymphs. Upon their transition to bimodal gas exchange, these groups diverge, with both showing additional increases in  $[\text{HCO}_3^-]$ , but with the aeshnid dragonflies maintaining their buffer capacity, while the buffer capacity of late-final libellulid nymphs undergoes a dramatic increase. This variation in the hemolymph non- $\text{HCO}_3^-$  buffer capacities between two families in the Anisoptera, and the large differences seen between dragonflies and other terrestrial insects, shows that this parameter varies widely within Insecta according to the insect's respiratory physiology, habitat and behavior. Finally, it remains to be seen whether the elevated  $P_{\text{CO}_2}$  and  $[\text{HCO}_3^-]$  observed in the hemolymph of secondarily aquatic dragonfly nymphs, relative to that of ancestrally water-breathing animals, is a trait specific to anisopterans, or whether this is a pattern that will be seen in water-breathing insects in general or even other secondarily aquatic animals.

## Acknowledgements

We thank the University of British Columbia Botanical Garden and Dolph Schluter for allowing us to collect dragonflies from in and around their ponds. We would also like to thank the two reviewers, whose constructive criticism greatly improved this paper.

## Competing interests

The authors declare no competing or financial interests.

## Author contributions

Conceptualization: D.J.L., P.G.D.M.; Methodology: D.J.L., P.G.D.M.; Validation: D.J.L.; Formal analysis: D.J.L.; Investigation: D.J.L.; Resources: D.J.L., P.G.D.M.; Writing - original draft: D.J.L.; Writing - review & editing: D.J.L., P.G.D.M.; Visualization: D.J.L., P.G.D.M.; Supervision: P.G.D.M.; Project administration: D.J.L., P.G.D.M.; Funding acquisition: P.G.D.M.

## Funding

This work was supported by the Natural Sciences and Engineering Research Council of Canada [Discovery grant: RGPIN-2014-05794 to P.G.D.M.].

## References

- Balian, E. V., L  v  que, C., Martens, K. and Segers, H. (2008). *Freshwater Animal Diversity Assessment*. Dordrecht, The Netherlands: Springer. doi:10.1007/978-1-4020-8259-7
- Boutilier, R. G., Heming, T. A. and Iwama, G. K. (1984). Physicochemical parameters for use in fish respiratory physiology. In *Fish Physiology*, Vol. 10 (ed. W. S. Hoar and D. J. Randall), pp. 403–430. Florida: Academic Press, Inc. doi:10.1016/S1546-5098(08)60323-4
- Bridges, C. R. and Scheid, P. (1982). Buffering and  $\text{CO}_2$  dissociation of body fluids in the pupa of the silkworm moth, *Hyalophora cecropia*. *Respir. Physiol.* **48**, 183–197. doi:10.1016/0034-5687(82)90079-2
- Buck, J. and Friedman, S. (1958). Cyclic  $\text{CO}_2$  release in diapausing pupae—III:  $\text{CO}_2$  capacity of the blood: carbonic anhydrase. *J. Insect Physiol.* **2**, 52–60. doi:10.1016/0022-1910(58)90027-1
- Corbet, P. S. (1962). *A Biology of Dragonflies*. London, UK: H. F. & G. Witherby Ltd.
- Erasmus, B. D. W., Howell, B. J. and Rahn, H. (1970). Ontogeny of acid-base balance in the bullfrog and chicken. *Respir. Physiol.* **11**, 46–53. doi:10.1016/0034-5687(70)90101-5
- Davenport, H. W. (1969). *The ABC of Acid-Base Chemistry: The Elements of Physiological Blood-Gas Chemistry for Medical Students and Physicians*. Chicago, US: The University of Chicago Press.
- de Pennart, A. and Matthews, P. G. D. (2019). The bimodal gas exchange strategies of dragonfly nymphs across development. *J. Insect Physiol.* doi:10.1016/j.jinsphys.2019.103982
- Gaino, E., Piersanti, S. and Rebora, M. (2007). Ultrastructural organization of the larval spiracles in *Libellula depressa* L. (Anisoptera: Libellulidae). *Odonatologica* **36**, 373–379.
- Garey, W. F. and Rahn, H. (1970). Normal arterial gas tensions and pH and the breathing frequency of the electric eel. *Respir. Physiol.* **9**, 141–150. doi:10.1016/0034-5687(70)90066-6
- Gulinson, S. L. and Harrison, J. F. (1996). Control of resting ventilation rate in grasshoppers. *J. Exp. Biol.* **199**, 379–389.
- Harrison, J. M. (1988). Temperature effects on haemolymph acid-base status *in vivo* and *in vitro* in the two-striped grasshopper *Melanoplus bivittatus*. *J. Exp. Biol.* **140**, 421–435.



- Harrison, J. M.** (1989). Temperature effects on intra- and extracellular acid-base status in the American locust, *Schistocerca nitens*. *J. Comp. Physiol. [B]* **158**, 763-770. doi:10.1007/BF00693015
- Harrison, J. F.** (2001). Insect acid-base physiology. *Annu. Rev. Entomol.* **46**, 221-250. doi:10.1146/annurev.ento.46.1.221
- Harrison, J. F., Hadley, N. F. and Quinlan, M. C.** (1995). Acid-base status and spiracular control during discontinuous ventilation in grasshoppers. *J. Exp. Biol.* **198**, 1755-1763.
- Heinrich, B. and Casey, T. M.** (1978). Heat transfer in dragonflies: 'fliers' and 'perchers'. *J. Exp. Biol.* **74**, 17-36.
- Heisler, N.** (1986). Buffering and transmembrane ion processes. In *Acid-Base Regulation in Animals* (ed. N. Heisler), pp. 3-47. Amsterdam: Elsevier Science Publishers B. V.
- Howell, B. J., Rahn, H., Goodfellow, D. and Herreid, C.** (1973). Acid-base regulation and temperature in selected invertebrates as a function of temperature. *Am. Zool.* **13**, 557-563. doi:10.1093/icb/13.2.557
- Iversen, N. K., Malte, H., Baatrup, E. and Wang, T.** (2012). The normal acid-base status of mice. *Resp. Physiol. Neurobiol.* **180**, 252-257. doi:10.1016/j.resp.2011.11.015
- Just, J. J., Gatz, R. N. and Crawford, E. C., Jr.** (1973). Changes in respiratory functions during metamorphosis of the bullfrog, *Rana catesbeiana*. *Respir. Physiol.* **17**, 276-282. doi:10.1016/0034-5687(73)90002-9
- Lee, D. J., Gutbrod, M., Ferreras, F. M. and Matthews, P. G. D.** (2018). Changes in hemolymph total CO<sub>2</sub> content during the water-to-air respiratory transition of amphibiotic dragonflies. *J. Exp. Biol.* **221**, jeb181438. doi:10.1242/jeb.181438
- Lenfant, C. and Johansen, K.** (1968). Respiration in the African lungfish *Protopterus aethiopicus*: I. respiratory properties of blood and normal patterns of breathing and gas exchange. *J. Exp. Biol.* **49**, 437-452.
- Levenbook, L.** (1950a). The physiology of carbon dioxide transport in insect blood: part I. the form of carbon dioxide present in *Gastrophilus* larva blood. *J. Exp. Biol.* **27**, 158-174.
- Levenbook, L.** (1950b). The physiology of carbon dioxide transport in insect blood: part III. The buffer capacity of *Gastrophilus* blood. *J. Exp. Biol.* **27**, 184-191.
- Matthews, P. G. D.** (2017). Acid-base regulation in insect Haemolymph. In *Acid-Base Balance and Nitrogen Excretion in Invertebrates: Mechanisms and Strategies in Various Invertebrate Groups with Considerations of Challenges Caused by Ocean Acidification* (ed. D. Weihrauch and M. O'Donnell), pp. 219-238. Cham: Springer International Publishing. doi:10.1007/978-3-319-39617-0\_8
- Nicholls, S. P.** (1983). Ionic and osmotic regulation of the haemolymph of the dragonfly, *Libellula quadrimaculata* (Odonata: Libellulidae). *J. Insect Physiol.* **29**, 541-546. doi:10.1016/0022-1910(83)90086-0
- Rockwood, J. P. and Coler, R. A.** (1991). The effect of aluminum in soft water at low pH on water balance and hemolymph ionic and acid-base regulation in the dragonfly *Libellula julia* Uhler. *Hydrobiologia* **215**, 243-250. doi:10.1007/BF00764859
- Stabenau, E. K. and Heming, T. A.** (1993). Determination of the constants of the Henderson-Hasselbalch equation, ( $\alpha$ ) CO<sub>2</sub> and pKa, in sea turtle plasma. *J. Exp. Biol.* **180**, 311-314.
- Sutcliffe, D. W.** (1962). The composition of haemolymph in aquatic insects. *J. Exp. Biol.* **39**, 325-344.
- Tillyard, R. J.** (1915). On the physiology of the rectal gills in the larvae of anisopterid dragonflies. *Proc. Linn. Soc. N.S.W.* **40**, 422-437. doi:10.5962/bhl.part.18879
- Truchot, J. P.** (1975). Blood acid-base changes during experimental emersion and reimmersion of the intertidal crab *Carcinus maenas* (L.). *Respir. Physiol.* **23**, 351-360. doi:10.1016/0034-5687(75)90086-9
- Weis-Fogh, T.** (1967). Respiration and tracheal ventilation in locusts and other flying insects. *J. Exp. Biol.* **47**, 561-587.
- Wootton, R. J.** (1988). The historical ecology of aquatic insects: an overview. *Palaeogeogr. Palaeoclimatol. Palaeoecol.* **62**, 477-492. doi:10.1016/0031-0182(88)90068-5